Methods

Preparation of isolated duodenal villi, pH_i measurements, calibration, and buffer capacity determination

For measuring pH_i in isolated duodenal villi, the duodenum was removed and immediately placed in ice-cold Ringer's solution (solution composition in mM: 147 NaCl, 4 KCl, 2.2 $CaCl_2$ within 500 μM DTT to prevent the mucus to clog the villi, pH 7.4). The duodenum was sliced into 0.5 cm sections and each section was opened along the mesenteric border. One piece of tissue was transferred onto the cooled stage of a dissecting microscope, and individual villi were detached from the intestine by snapping off the duodenal base with sharpened microdissection tweezers. Care was taken not to damage the apical part of the villi. The villi were attached to a glass coverslip precoated with Cell-Tak adhesive (BD Biosciences, Bedford, MA, USA). Intracellular buffering capacity (βi) of duodenal villi was determined as described (2, 3). Briefly, the duodenal villi were perfused with a Na^+ and HCO_3^--free solution (using TMA^+ instead of Na^+ in Buffer A: 120 NaCl, 10 HEPES, 5 Tris, 2.25 KH_2PO_4, 1.5 K_2HPO_4, 1.2 $MgSO_4$, 1.2 Ca-Gluconate, 10 glucose, pH7.4) containing varying concentrations of NH_4Cl. For each NH_4Cl addition, β_i was determined as $\Delta[NH4^+]_i/\Delta pH_i$, where $[NH4^+]_i$ is $[NH3]_i \times 10^{pKa-pHi}$. $[NH3]_i=[NH3]_o=[NH4^+]_o \times 10^{pHo-pKa}$. pH_i and pH_o were measured, $[NH4^+]_o$ was known, and pKa at 37°C is 8.9. There were no apparent differences in β_i among different backgrounds of murine duodenal villi. The total buffering capacity (β_{total}) was calculated from the equation: $\beta_{total}=\beta_i+\beta_{HCO3-}=\beta_i+2.3\times s\times Pco_2\times 10^{pHi-pKa}$, where solubility of CO_2 in cell cytoplasm (we used the value for blood) and pKa is 6.36 at HCO_3^-/CO_2. Isolated individual villi were loaded for approx. 10min with 16 μM 2',7'-bis(2-carboxyethyl)-5(6)-carboxy-fluorescein acetoxymethyl ester BCECF-AM (Molecular Probes, Leiden, The Netherlands) in Ringer's solution at room temperature. After being loaded, the villi were fixed on the coverslip with a polycarbonate membrane (25 mm diameter, pore size

3 μm, Osmonics, Minnetonka, MN, USA) in a custom-made perfusion chamber, mounted onto the heated (37 °C) stage of an inverted microscope (Zeiss Axiovert 200, Carl Zeiss AG, Jena, Germany). NHE3 activity was measured by NH_4^+ prepulse technique. The BCECF-loaded villi were perfused with prewarmed (37 °C) O_2-gassed buffer A for 20min for a stable baseline reading. Villi were acidified using an ammonium prepulse (40 mM NH_4Cl isotonically replacing NaCl) for 7 min, then perfused for 4 min with a Na^+-free buffer A (TMA^+ isotonically replacing Na^+), until pH_i reached its lowest value plateau. Subsequently, 50 μM HOE642 (to eliminate NHE1 and NHE2 activity (1), or 50 μM HOE642 with 20 μM S1611 (To inhibit NHE3 activity as well) was added to the Na^+-free buffer A. After 2 min, the buffer was switched to Na^+-containing buffer B, containing 50 μM HOE642 or 50 μM HOE642 with 20 μM S1611 to eliminate the contributions of NHE1 and NHE2, or NHE1-3. Cl^-/HCO_3^- exchange rate was accessed as changes in intracellular pH after removing Cl^- from perfusion buffer. The villi were perfused with prewarmed (37 °C) 5 %CO_2-gassed buffer B (solution composition in mM: 98 NaCl, 22 $NaHCO_3$, 10 HEPES, 5 Tris, 2.25 KH_2PO_4, 1.5 K_2HPO_4, 1.2 $MgSO_4$, 1.2 Ca-Gluconate, 10 glucose, pH 7.4) for 20min. for a stable baseline reading. Villi were alkalised by removing chloride (Na-gluconate isotonically replacing NaCl) until stabilized. And then the intracellular pH was back by giving back chloride in the perfusion buffer. The images were digitalized 30s with a cooled CCD camera (CoolSnap ES, Roper Scientific, Ottobrunn, Germany) using the Metafluor software (Universal Imaging Corporation, Downington, PA, USA) during exposure of cells to alternating 440 and 495 nm light from a monochromator (Visichrome, Visitron Systems, Puchheim, Germany) with a 515 nm DCXR dichroic mirror and a 535 nm barrier filter (Chroma Technology Corp, Rockingham, VT, USA) in the emission pathway. Individual regions of interest (ROIs) at the tip of the villi were outlined and monitored during the course of the measurement. The rates of pH_i change measured in the experiments were converted to proton flux using the equation $J_{H+}=\Delta pH/\Delta t \times \beta_{total}$. Approx. two to three villi were measured per experiment, and the results of

these flux measurements averaged for each mouse. *n* is the number of mice that were used for each individual data bar. The 440/495 time course was reproduced from the stored images after background subtraction. Calibration of the 440/495 ratio was performed using the high K^+-nigericin method (solution composition in mM: 100 potassium gluconate, 20 KCl, 20 NaCl 10 HEPEPS, 2.25 KH_2PO_4, 1.5 K_2HPO_4, 1.2 calcium gluconate, 1.2 $MgSO_4$, 10 glucose, 10μM nigericin, pH 7.4). In a second step, the steady-state pH_i in the presence of CO_2/HCO_3^- was determined by measuring the ratio under steady-state conditions, then performing a two-point calibration at pH 7.2 and 7.6, two values that we expected to be slightly below and above the estimated steady-state pH_i.

Reference

1. **Bachmann O, Riederer B, Rossmann H, Groos S, Schultheis PJ, Shull GE, Gregor M, Manns MP, Seidler U**. The Na+/H+ exchanger isoform 2 is the predominant NHE isoform in murine colonic crypts and its lack causes NHE3 upregulation. Am J Physiol Gastrointest Liver Physiol 287: G125-133, 2004.

2. **Bachmann O, Rossmann H, Berger UV, Colledge WH, Ratcliff R, Evans MJ, Gregor M, Seidler U**. cAMP-mediated regulation of murine intestinal/pancreatic Na+/HCO3- cotransporter subtype pNBC1. Am J Physiol Gastrointest Liver Physiol 284: G37-45, 2003.

3. **Roos A, Boron WF**. Intracellular pH. Physiol Rev 61: 296-434, 1981.

Figure legends

Figure 1: The effect of S1611 on acid-activated Hoe642 insensitive proton extrusion rate in duodenal and jejunal villous enterocytes. (**A)** BCECF-stained microdissected duodenal villi. **(B)** Representative pH trace during the measurement of the buffer capacity by stepwise decrease and increase of the NH_4^+ concentration. **(C)** Total and intrinsic buffering capacity of the pinched villi from the duodenum and jejunum. **(D)** Representative pH_i trace of an NH_4^+ prepulse experiment that measures the effect of S1611 on NHE3 activity in microdissected duodenal villi. **(D)** Effect of 20 µM S1611 on acid-activated Hoe642-insensitive proton extrusion rate in duodenal and jejunal villi. 40 µM did not cause a stronger inhibition than 20 µM (data not shown). n = 5, 3-5 individual experiments per mouse.

Figure 2: Effect of S1611 on steady-state pH_i and Cl^-/HCO_3^- exchange rates in microdissected duodenal villi. **(A)** S1611 caused a short lasting pH_i increase in duodenal villus enterocytes. This pH_i increase was not observed when S1611 was added when the cells were acidic, during the NH_4^+ prepulse experiment shown in Figure 1. Subsequent Cl^- removal resulted in a slightly higher alkalinization than in duodenocytes not pretreated with S1611, but the Cl^- re-addition caused a pH_i decline of similar speed and magnitude. Thus, no indication for an increase of a long lasting Cl^-/HCO_3^- exchange rate was found in the experiments. n= 3, several individual experiments per mouse.

Figure 3: Effect of the CFTR(inh)-172 on forskolin-stimulated duodenal HCO_3^- secretion during Cl^- free luminal perfusion in vivo. The duodenal lumen of anethetized mice was perfused with Cl^- free-solution to inhibit Cl^-/HCO_3^- exchange-mediated HCO_3^- secretion. 10^{-4} M forskolin in the luminal perfusate induced a robust secretory response even the absence of luminal Cl^-, and the CFTR(inh)-172 inhibited >50% of the overall HCO_3^- output. Thus, the

inhibitor is reasonably active even with maximal CFTR activation and maximal driving force for electrogenic anion secretion.

Figure 4: Relative mRNA expression of CFTR, NHE3, Slc26a6 and Slc26a3 in the murine duodenum. The qPCR was performed in WT mice against β-actin **(A)** and cytokeratin 18 **(B)** as control genes. CFTR and NHE3 showed similar expression levels with any of the control genes, and Scl26a3 and Slc26a6 showed higher expression levels.

Figures

Figure 1

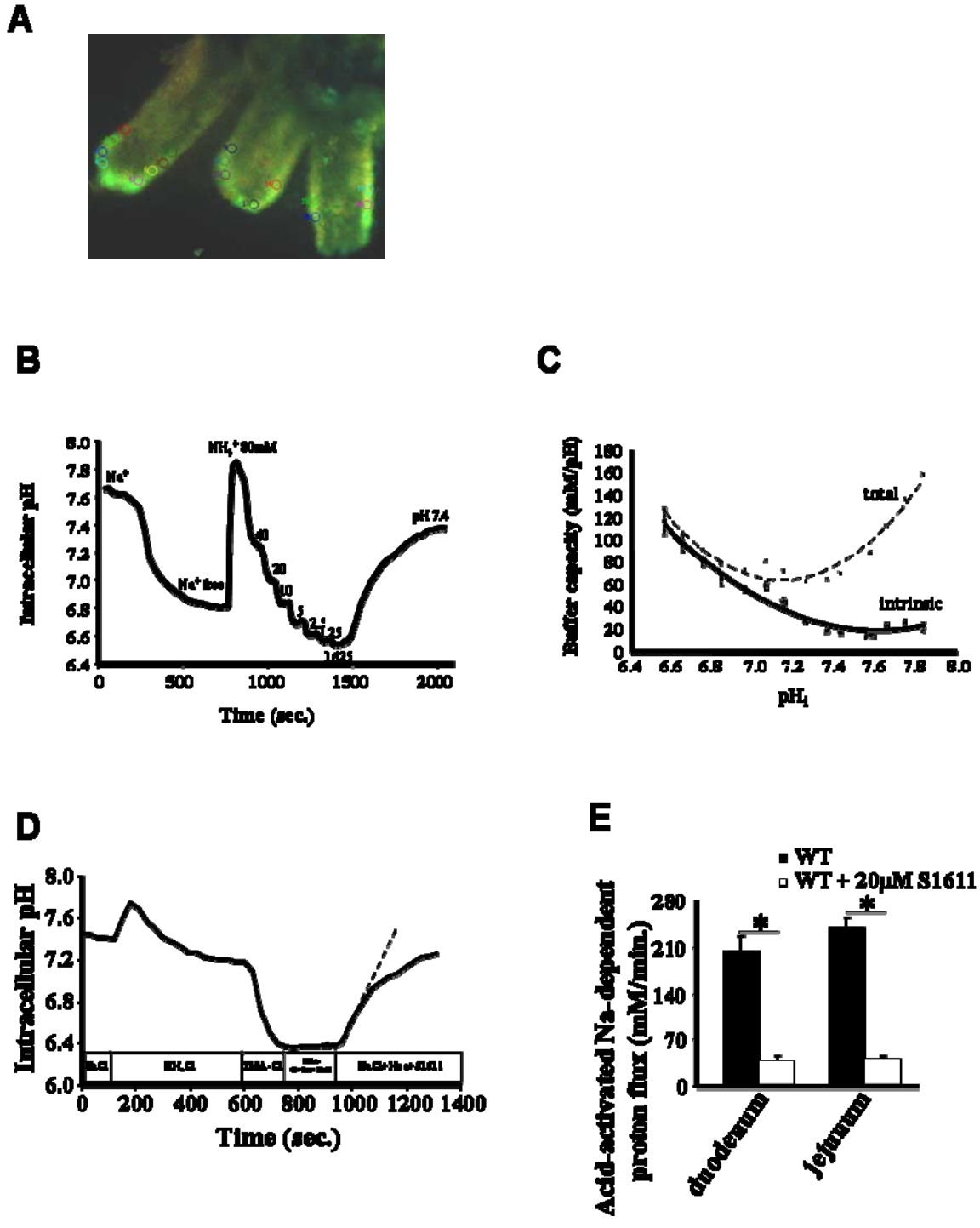

Figure 2

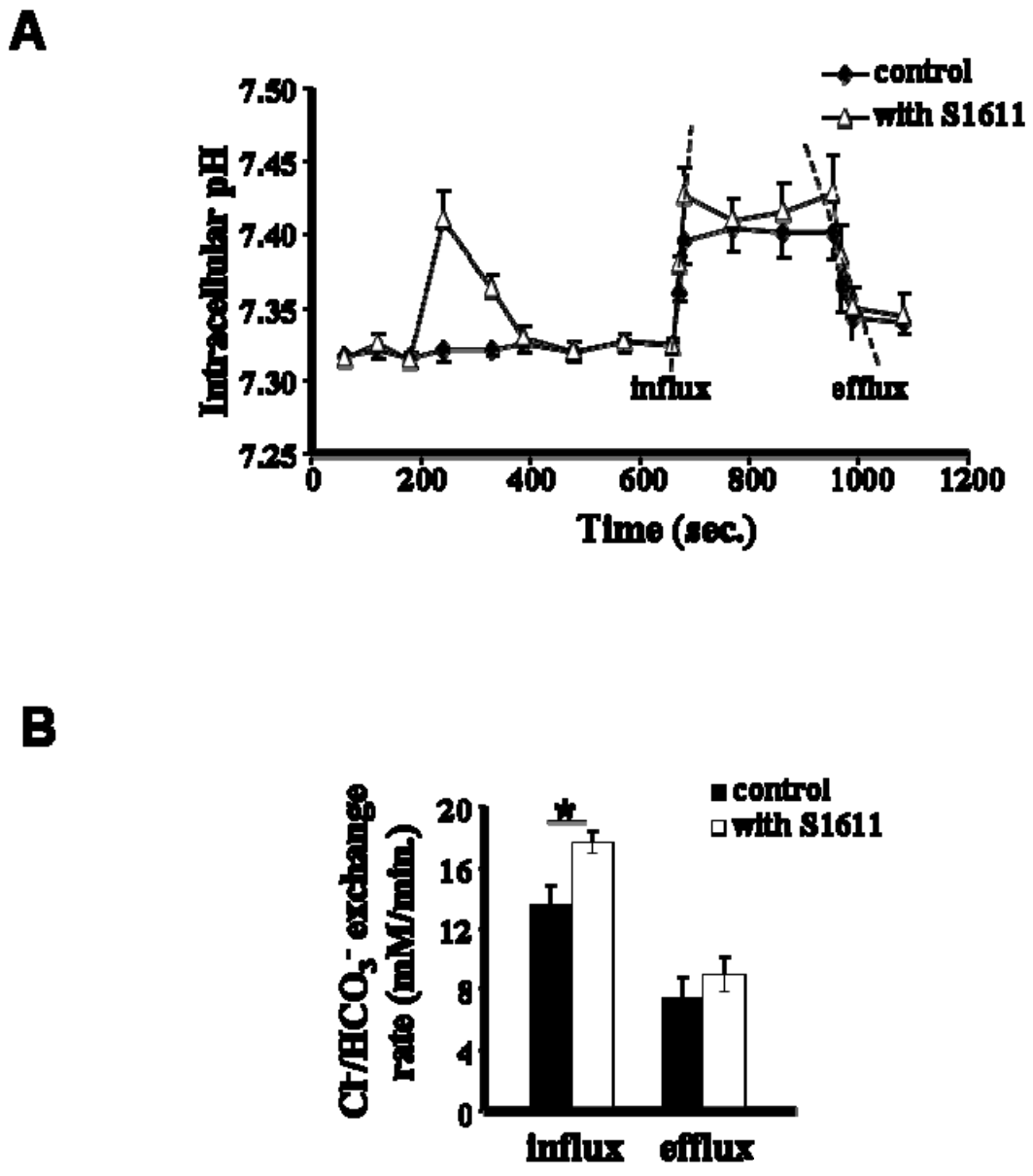
A
control
with S1611
Intracellular pH
7.50
7.45
7.40
7.35
7.30
7.25
influx
efflux
0
200
400
600
800
1000
1200
Time (sec.)
B
control
with S1611
Cl-/HCO3- exchange rate (mM/min.)
20
16
12
8
4
0
*
influx
efflux

Figure 3

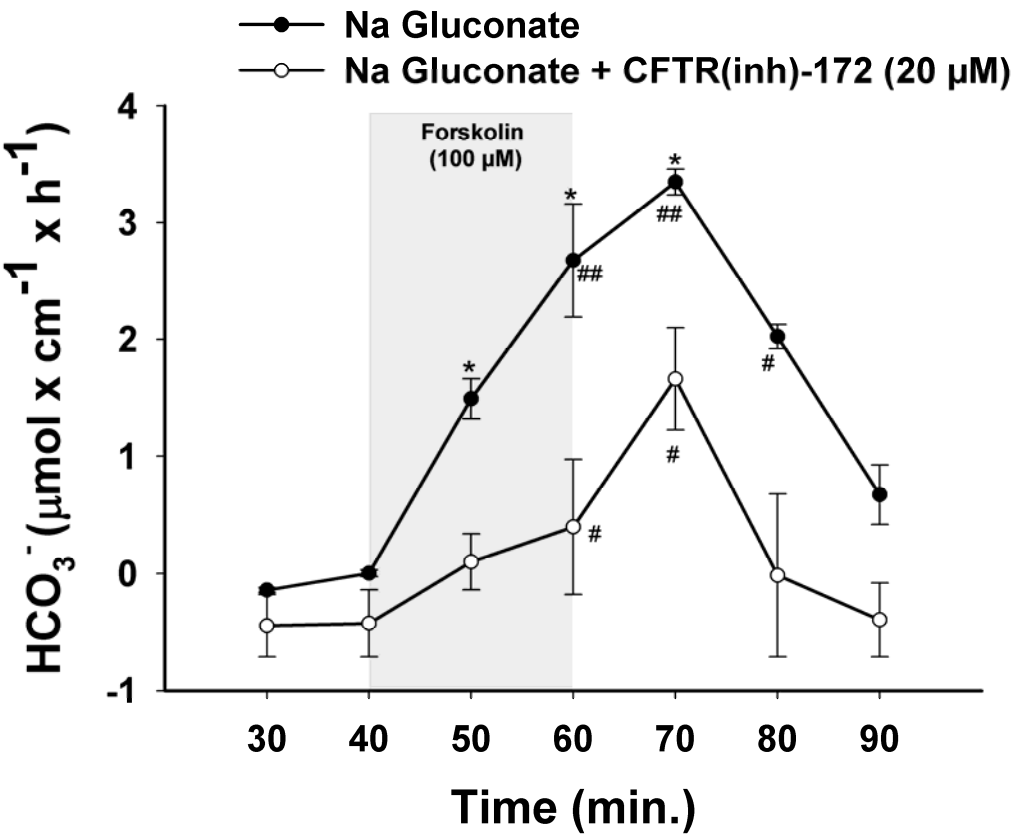
Na Gluconate
Na Gluconate + CFTR(inh)-172 (20 µM)
Forskolin
(100 µM)
HCO3- (µmol x cm-1 x h-1)
Time (min.)
4
3
2
1
0
-1
30
40
50
60
70
80
90
*
##
#

Figure 4:

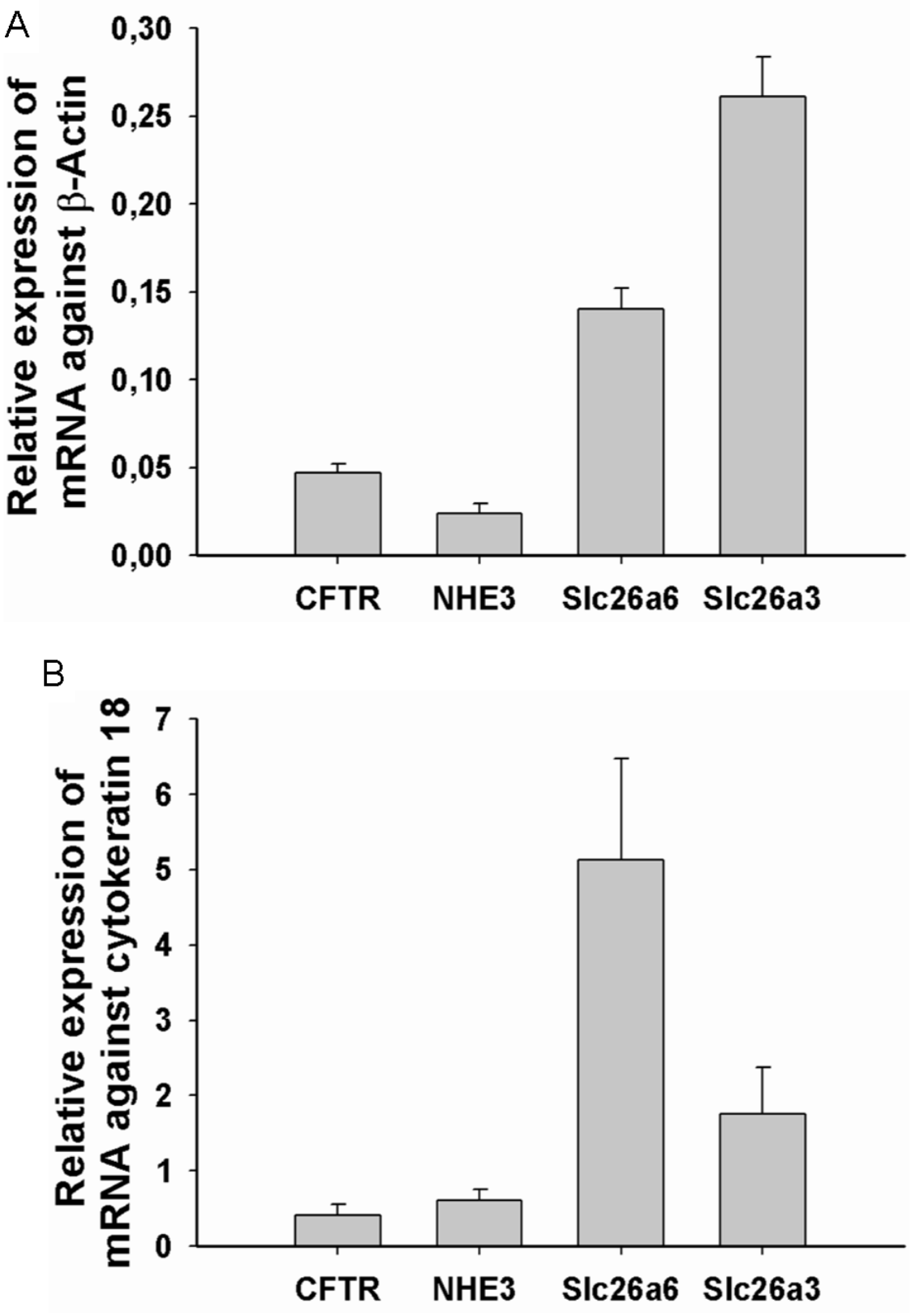
A
Relative expression of mRNA against β-Actin
0,30
0,25
0,20
0,15
0,10
0,05
0,00
CFTR
NHE3
Slc26a6
Slc26a3
B
Relative expression of mRNA against cytokeratin 18
7
6
5
4
3
2
1
0
CFTR
NHE3
Slc26a6
Slc26a3